Available online at www.sciencedirect.com

SciVerse ScienceDirect

Ceramics International 39 (2013) 597–603

CERAMICS INTERNATIONAL

www.elsevier.com/locate/ceramint

Effects of heat-treatment temperature and starting composition on morphology of boron carbide particles synthesized by carbothermal reduction

Tomohiro Kobayashi[a,*], Katsumi Yoshida[b], Toyohiko Yano[b]

[a]*Department of Nuclear Engineering, Tokyo Institute of Technology, 2-12-1, O-okayama, Meguro-ku, Tokyo 152-8550, Japan*
[b]*Research Laboratory for Nuclear Reactors, Tokyo Institute of Technology, 2-12-1, O-okayama, Meguro-ku, Tokyo 152-8550, Japan*

Received 3 April 2012; received in revised form 22 June 2012; accepted 22 June 2012
Available online 28 June 2012

Abstract

Carbothermal reduction using B_2O_3 and carbon black was applied for synthesis of B_4C powder and the effects of heat-treatment temperature and starting composition of raw mixture on morphology of B_4C particles were investigated. Morphology of B_4C particles synthesized at 1450 °C was mainly spherical shapes. The B_4C powder synthesized at 1550 °C was large and changed in morphology from polyhedral to skeletal shape, and particle size of B_4C increased with an increase in the amount of B_2O_3 in the starting mixtures. The B_4C powder synthesized beyond 1650 °C consisted from dendrite-like particles aggregated by small primary particles. Morphology of the primary B_4C particles synthesized at 1750 °C changed from polyhedral to rounded shape with increasing the amount of B_2O_3 in the starting mixtures. It is clarified that heat-treatment temperature and the starting compositions of raw mixtures mainly affected B_4C nuclei number along with primary particle size and morphology of primary B_4C particles, respectively.

Keywords: A. Grain growth; A. Crystal morphology; B. Grain size; D. Carbides

1. Introduction

Boron carbide (B_4C) has excellent properties such as light weight, superior hardness, high elastic modulus, high thermal stability and large neutron absorption cross section, and B_4C has been used for armor materials, wear-resistance parts, grinding media and neutron absorber of control rods for nuclear fission reactors [1]. In addition, B_4C has a potential as a reinforcement to improve mechanical properties of ceramics and metals because of its excellent mechanical properties.

In ceramics fields, ceramic powder with various morphology, such as fiber, whisker, nanowire and polyhedral particles (platelets, prisms and rods), have been used as reinforcements for ceramic matrix composites. Recently, B_4C nanowires [2–4] and whiskers [5,6] were successfully synthesized by CVD, VLS and carbon nanotube template method. On the synthesis of polyhedral B_4C powder, it was synthesized by carbothermal reduction (CTR) method [7–10], sol-gel method [11,12] and borate precursor method [13–16]. In particular, it was reported that B_4C powder synthesized by CTR using B_2O_3 and carbon sources contained B_4C platelets and prisms [7–9], and B_4C powder synthesized by sol-gel and borate precursor method showed aggregates consisted of small polyhedral B_4C particles [11].

CTR method using B_2O_3 and carbon is expected to be suitable for synthesis of polyhedral B_4C powder from previous studies [7–10]. CTR is expressed by overall reaction of (1) and step reactions of (2) and (3). Up to now, there are several researches for B_4C synthesis using B_2O_3 and various carbon sources, such as carbon black [7–9], active carbon [9] or cornstarch [10]. However, these studies focused on reduction of residual carbon and synthesis of B_4C powder at lower heat-treatment temperature. Hence, there are very few studies on the effect of synthesis conditions on the morphology of B_4C powder

*Corresponding author. Tel.: +81 3 5734 3082.
E-mail address: kobayashi.t.bc@m.titech.ac.jp (T. Kobayashi).

0272-8842/$36.00
http://dx.doi.org/10.1016/j.ceramint.2012.06.070

and the growth mechanism of polyhedral B_4C particles. Present authors paid attention to morphological change of B_4C powder by change in heat-treatment temperature and starting composition of raw mixture.

$$2B_2O_3 + 7C \rightarrow B_4C + 6CO \quad (1)$$

$$B_2O_3 + 3C \rightarrow 2B + 3CO \quad (2)$$

$$4B + C \rightarrow B_4C \quad (3)$$

In this study, CTR using B_2O_3 and carbon black was applied for the synthesis of B_4C powder and the effects of heat-treatment temperature and composition of raw mixtures on morphology of synthesized B_4C powder were investigated.

2. Materials and methods

B_2O_3 (boron tri-oxide, 97% purity; Kanto Chemical Co. Inc., Japan) and carbon black (denoted as CB, Asahi Thermal, average particle size: 80 nm; Asahi Carbon Co. Ltd., Japan) were used as starting materials. The composition of powder mixtures and heat-treatment temperature are listed in Table 1. B_2O_3 and CB powders were mixed by dry ball-milling in plastic bottle with polyethylene resin balls for 2 h. The weight ratio of B_2O_3/C for stoicheometry in the reaction (1) is 1.66, which was denoted as 7C. B_2O_3 changes from a solid to a liquid phase at 480 °C, and B_2O_3 exists as liquid during heat-treatment. Because B_4C particles may grow from liquidus phase, morphology of B_4C particles probably depends on the amount of B_2O_3 in the raw mixture. Furthermore, evaporation of B_2O_3 during heat-treatment was also expected. Therefore, B_2O_3 rich compositions were prepared. The weight ratios of B_2O_3/C in B_2O_3-rich compositions were 2.32 and 3.87, which were denoted as 5C and 3C, respectively (Table 1).

Powder mixture was pressed into compacts at 30 MPa by uniaxial pressing, and they were put into a graphite crucible. Compacts were heat-treated at 1450–1750 °C for 3 h at a heating rate of 30 °C/min in argon (Ar) gas flow (2 *l*/min) using a graphite heater furnace (Hi-Multi 5000; Fuji Dempa Kogyo Co. Ltd., Japan). For comparison, B_4C was also synthesized at 1550 °C by solid-state reaction (SSR) based on the reaction (3) from boron (B, average grain size: 1.6 μm; Hirano Seizaemon Co. Ltd., Japan) and CB under the same heating condition. Weight change of B_2O_3 and CB mixtures up to 500 °C was measured by thermogravimetry-differential thermal analysis (TG-DTA, TG-DTA2020SA, Bruker AXS, Japan) under Ar gas flow (flow rate: 100 m*l*/min). Crystalline phases of the powder synthesized in this study were identified by X-ray diffractometry (XRD, PW-1700, Philips, the Netherlands) using monochromated CuKα radiation. Morphology of the powder was observed with a scanning electron microscope equipped with a field emission gun (FE-SEM, S-4800; Hitachi High-Technologies Corporation, Japan). Before SEM observation of the product heat-treated at 1450 °C, residual B_2O_3 and carbon were removed by hot water and decantation in ethanol, respectively. Particle size of the B_4C powder was measured using SEM micrographs.

Table 1
Compositions of powder mixtures and their processing conditions.

Sample code	Reactants	B_2O_3/C weight ratio	Heat-treatment temperature/°C
7C	B_2O_3, CB	1.66	1450–1750
5C	B_2O_3, CB	2.32	1450–1750
3C	B_2O_3, CB	3.86	1450–1750
B-C	B, CB		1550

3. Results and discussion

Fig. 1(a) shows XRD patterns of the raw mixture (7C composition) and the powders synthesized at 1450–1750 °C for 3 h. The strongest diffraction peak for B_4C appeared at an diffraction angle of 37.8° (2θ) in the powder after heat-treatment at 1450 °C. Diffraction peaks corresponding to residual B_2O_3 disappeared in the powders synthesized at 1550–1750 °C, and the amount of residual carbon slightly decreased with increasing heat-treatment temperature. This was probably attributed to an increase in reactivity of the reaction (1) with increasing heat-treatment temperature. XRD patterns of the raw mixture (3C composition) and the powder synthesized at 1450–1750 °C were shown in

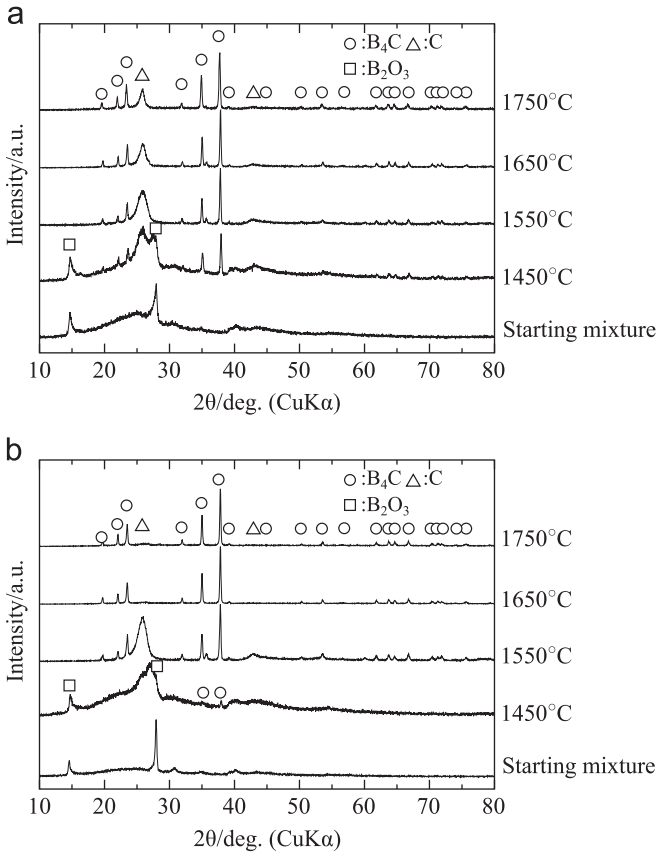

Fig. 1. XRD patterns of starting mixture and products after heat-treatment at 1450–1750 °C for 3 h using (a) 7C mixture and (b) 3C mixture.

Fig. 1(b). As shown in Fig. 1(b), peak intensity derived from residual carbon of the powder using 3C composition also decreased as increase in heat-treatment temperature, and the amount of residual carbon reduced to almost negligible after the heat-treatment at 1650 and 1750 °C both in 3C and 5C compositions. The amount of residual carbon in the products heat-treated at 1550 °C using 7C, 5C and 3C mixtures were almost same. XRD pattern of the powder product synthesized at 1550 °C by SSR using B and CB also indicated formation of crystalline B_4C, as shown in Fig. 2. By SSR, the amount of residual carbon in the reaction products was less than that by CTR of the same heat-treatment temperature.

Table 2 shows expected weight loss of the stoichiometric reaction (1) and observed weight loss of the 7C, 5C and 3C powder after each heat-treatment. The reaction (1) indicates that weight loss caused by CO gas evolution should be related to the production of B_4C. The weight losses of the samples heat-treated at 1450 °C decreased with increasing amount of B_2O_3 of the starting mixture. At 1450 °C, evaporation rate of B_2O_3 may be slow and weight loss was mainly caused by the formation of B_4C. From Fig. 1, the amount of B_4C of 7C composition was larger, and residual B_2O_3 of 7C composition was smaller than those of 3C composition, therefore the weight loss decreased with increasing amount of B_2O_3 in starting mixtures. The measured weight loss increased in the range of 1450–1550 °C by acceleration of the reaction (1) and evaporation of B_2O_3. The weight losses of samples with the same raw composition were almost constant at 1550–1750 °C. In order to confirm this, changes in weight losses of the samples (7C and 3C) were calculated from an amount of synthesized B_4C and the reaction equation (4), which is a modification of (1),

$$2B_2O_3 + 7C \rightarrow xB_4C + 6xCO\uparrow + 2(1-x)B_2O_3\uparrow + 7(1-x)C \quad (4)$$

where x is less than 1. Amount of B_4C was estimated from the XRD peak intensity of the products using a standard calibration curve. Calculated weight loss as a function of the heat-treatment temperature (1550–1750 °C) is shown in Fig. 3(a) and (b). The calculated overall weight losses (sum of weight loss of B_2O_3 and CO) were slightly lower than those of the samples observed experimentally. This difference could be attributed for the weight loss of the raw mixtures derived from dehydration of H_3BO_3 formed on B_2O_3 powder surface. Dehydration was indicated as endothermic peaks around 100 and 150 °C in TG-DTA measurement (Fig. 4). As shown in Fig. 3, the weight losses at 1550 °C derived from volatilization of B_2O_3 were greater than those at 1650 and 1750 °C in both composition, and markedly larger in the boron-rich composition (3C). This indicates that B_2O_3 evaporates as probably B-O species (mainly B_2O_3 and B_2O_2 gas [17]) during heating, and particularly in the B_2O_3-rich compositions. They did not contribute to produce B_4C. The percentage of CO gas

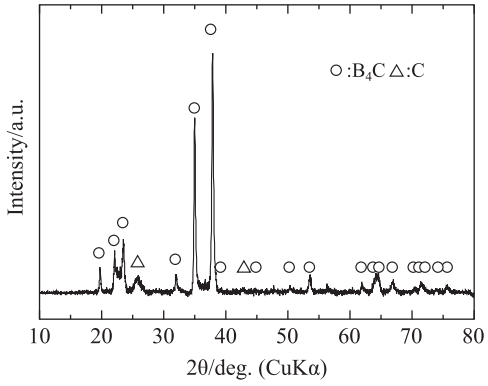

Fig. 2. XRD pattern of the product after heat-treatment using B-C mixture at 1550 °C for 3 h.

Table 2
Expected weight loss of the reaction (1) and observed weight loss of the samples after heat treatment.

Heat-treatment temperature/°C	Weight loss/wt%		
	7C	5C	3C
1450	55.5	42.8	23.2
1550	75.7	84.6	90.9
1650	79.9	86.3	89.7
1750	75.4	84.4	90.6
Expected loss	75.3		

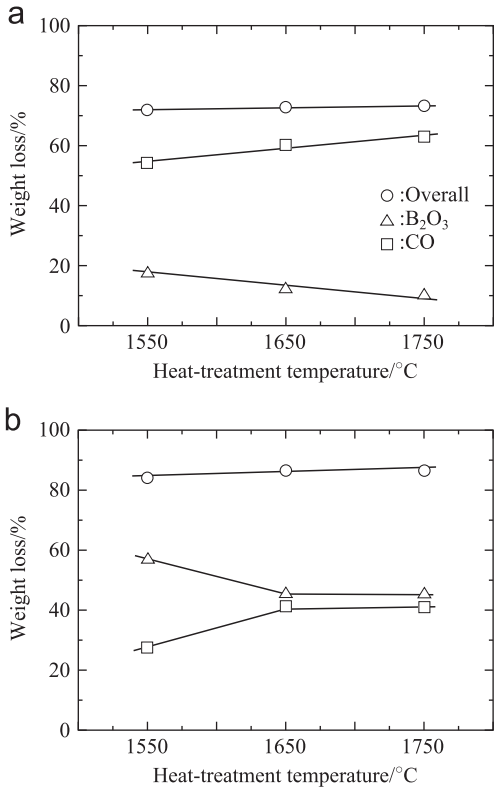

Fig. 3. Calculated weight losses as a function of the heat-treatment temperature. (a) 7C and (b) 3C composition.

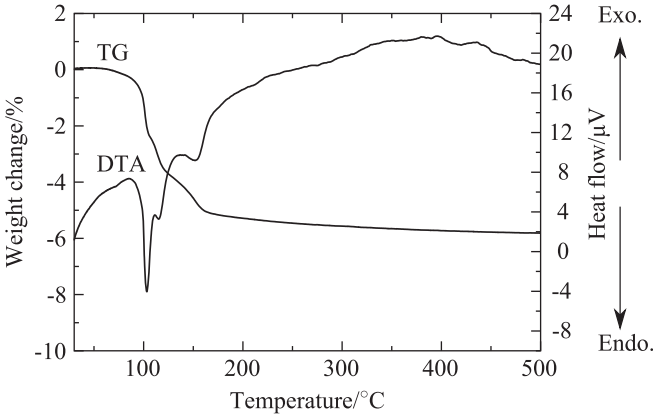

Fig. 4. TG-DTA curve for powder mixture of 7C composition.

contributing to the weight losses increased, and volatilization loss of B_2O_3 decreased with increasing heat-treatment temperature, because reactivity of CTR increased with an increase in the heat-treatment temperature. In addition, overall weight change slightly increased with increasing heat-treatment temperature but percentage of increase was very small, since the reaction (1) was completed and excess B_2O_3 was fully evaporated at higher temperature than 1550 °C. No residual B_2O_3 was observed as shown in Fig. 1.

Fig. 5(a)–(c) shows SEM micrographs of the powder synthesized from the 7C mixture and heat-treated at 1450 °C. The powder consisted of aggregates of small spherical particles (Fig. 5(a) and (b)) and rarely polyhedral particles with a particle size of about 30 μm (Fig. 5(c)). In Fig. 5(b), polyhedral shaped grains with a particle size of 2−3 μm are also observed. Morphology and particle size of the powder heat-treated at 1450 °C using B_2O_3-rich compositions were not so different from those of the powder using 7C composition.

SEM micrographs of the B_4C powder synthesized at 1550 °C using the 7C and the 3C mixture are shown in Fig. 6(a) and (b), respectively. Primary particle size of the B_4C powder using the 7C mixture is 44 μm, measured along the maximum length axis (Fig. 6(a)). This value is comparable with the particle size of B_4C powder using CB reported in Ref. [9]. Morphology of the B_4C particles was mainly polyhedral and partially thick plate-like in the case of 7C composition. Most of the B_4C synthesized from the 3C mixture (Fig. 6(b)) showed skeletal particles and had larger particle size (53 μm), as compared with that of 7C composition (Fig. 6(a)). B_4C powder using the 5C powder mixture consisted of polyhedral and skeletal particles with a particle size of 46 μm. The B_4C particles synthesized at 1550 °C using all compositions were not aggregated. These changes in morphology and particle size were probably resulted from the increase in B_2O_3 liquid. During the heat-treatment of the 3C mixture at 1550 °C, needle and blade-like B_4C were also grown from wall or limb of the graphite crucible. These needle and blade-like particles were grown

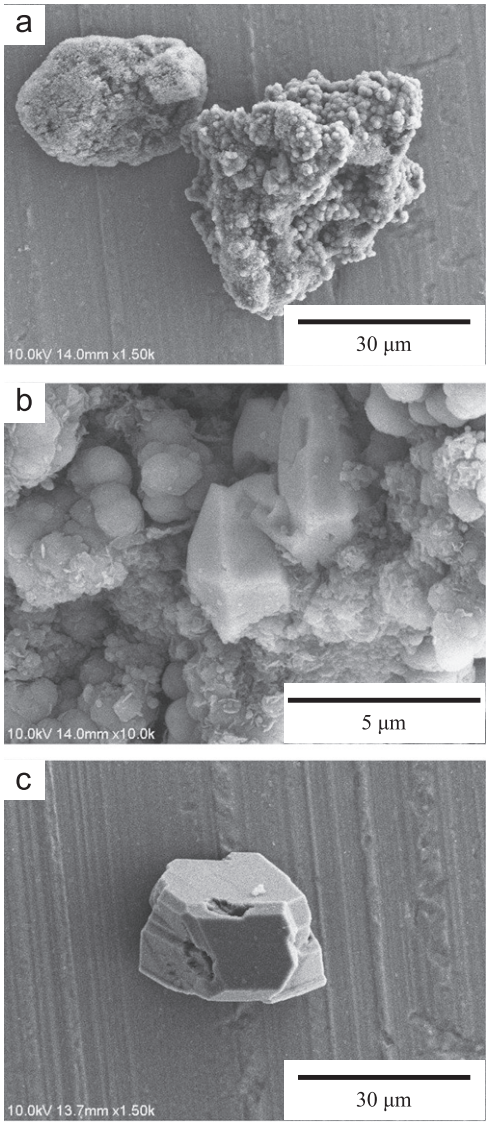

Fig. 5. SEM micrographs of the powder synthesized at 1450 °C for 3 h using 7C composition. (a) irregular aggregates, (b) magnify of (a) and (c) polyhedral particle.

by vapor–liquid–solid growth [5,6], so that evaporation of the raw materials, particularly B_2O_3, was confirmed.

The effect of B_2O_3 liquid on the growth of B_4C particles could be also observed by comparison of morphology and particle size of B_4C synthesized by CTR and SSR. SEM micrograph of B_4C powder synthesized at 1550 °C by the reaction (3) is shown in Fig. 6(c). The B_4C particles showed irregular shape and the particle size was 2−3 μm, which was much smaller than that of the B_4C powder synthesized by CTR using B_2O_3 and CB mixtures at 1550 °C. It indicates that B_2O_3 worked as flux, and supported growth of crystals. Large amount of flux, i.e., B_2O_3-rich composition, caused larger crystals, since there was a longer time for crystal growth until dried up of the flux.

Fig. 7(a) shows SEM micrograph of B_4C powder synthesized at 1650 °C using 7C mixture. Morphology of the B_4C powder synthesized at 1650 °C for all starting

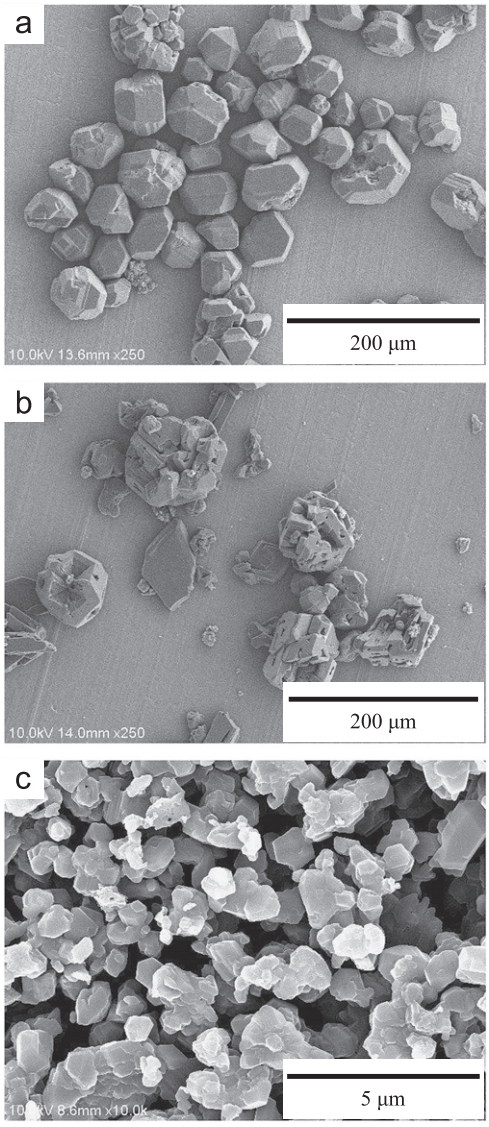

Fig. 6. SEM micrographs of B_4C powder synthesized at 1550 °C for 3 h using (a) 7C composition, (b) 3C composition and (c) B-C mixture.

compositions was dendrite-like shape formed by aggregation of small B_4C particles, and its primary particle size was 7−9 μm. It is noted that primary particle size of B_4C powder drastically decreased with increasing heat-treatment temperature from 1550 °C to 1650 °C.

SEM micrographs of B_4C powder synthesized at 1750 °C using the 7C and 3C mixture are shown in Fig. 7(b) and (c), respectively. Dendrite shape of the B_4C powder was commonly observed and it should be generated by nucleation of several smaller primary B_4C particles. Primary particle size of B_4C synthesized using the 7C and 3C mixture was 6 μm and 5 μm, respectively. Morphology of primary particles synthesized at 1750 °C changed from polyhedral with clear edges to rounded shapes with an increase in the amount of B_2O_3 in the starting mixtures (Fig. 7(b) and (c)). In order to investigate this morphology change, the B_4C powder synthesized at 1550 °C (7C) was further heat-treated at 1750 °C with addition of 10 wt% B_2O_3. Edges of polyhedral B_4C particles were rounded off by the heat-treatment with B_2O_3 (Fig. 7(d)). The weight loss of this powder due to the heat-treatment at 1750 °C was 12.4 wt%. This value was 2.4 wt% larger than the weight of additional B_2O_3. The explanation for this was that the small amount of B_4C on the surface of the powder reacted with liquid B_2O_3 at high temperatures. Derkach et al. reported that B_2O_2 gas mainly generated by heat-treatment of B_4C + 3 wt.% B_2O_3 mixture at 900–1100 °C [18]. Whereas the temperature range in their study was much lower than that in this study, B_2O_2 gas might be produced mainly by the reaction between B_4C and B_2O_3 at 1750 °C.

According to the study on kinetics of CTR for synthesis of B_4C using B_2O_3 and cornstarch at a temperature range of 1530–2100 °C, Weimer et al. reported that an increase in nucleation-growth rate coefficients for B_4C synthesis corresponded with decrease in particle size of B_4C powder at around 1700 °C [10]. Our results agree with their results. Large nucleation-growth rate should result in rapid production of numerous B_4C nuclei, and result in relatively small primary particle size. In this study, large transient was observed between 1550 and 1650 °C. Change in intensity ratio $I_{B4C}/(I_{B4C} + I_C)$ of the strongest XRD peaks of the products as a function of the heat-treatment temperature is shown in Fig. 8. The intensity ratio increased with increasing heat-treatment temperature. Below 1550 °C, the intensity ratio of each compositions was not so different. However, beyond 1650 °C, the value of the intensity ratios of the B_2O_3-rich compositions (5C and 3C) was almost 1.0. This means that the B_4C formation reaction was completed at 1650 °C in 5C and 3C compositions in short time less than 3 h (keeping period), since there is no residual B_2O_3 and C. The quick generation of B_4C should be related to the simultaneous nucleation of large number crystals resulting in smaller primary grains. An excess B_2O_3 contributes to growth of B_4C particles at less than 1550 °C, but has no significant effect at higher temperatures due to short remaining period. On the contrary, in the 7C composition, formation of B_4C was limited due to the deficient of B at 1650 and 1750 °C. At these temperatures, residual C was detected in XRD patterns as shown in Fig. 1(a). Based on the results shown in Fig. 8, it is clear that formation reaction of B_4C proceeds mostly in advance of evaporation of B_2O_3 or decomposition of B_4C.

In summary, morphology of B_4C powder synthesized by CTR using B_2O_3 and CB strongly depended on the heat-treatment temperature and the starting compositions of powder mixture. The B_4C powder with polyhedral morphology and large particle size was resulted from the heat-treatment at 1550 °C. In the case of B_2O_3-rich mixtures and the heat-treatment at 1550 °C, morphology of the B_4C particles changed to skeletal shape. The dendrite-like B_4C powder agglomerated by small primary particles was obtained by heat-treatment at higher temperatures. This was resulted from increase in B_4C nuclei number with an

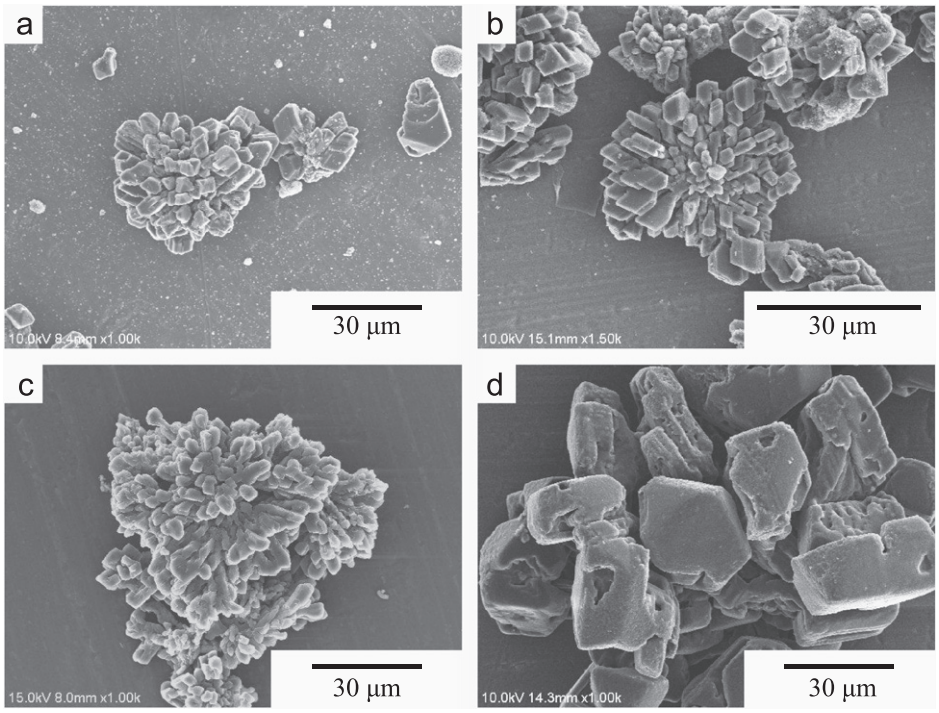

Fig. 7. SEM micrographs of the product heat-treated at (a) 1650 °C using 7C composition, 1750 °C using (b) 7C composition and (c) 3C composition. SEM micrograph of (d) the B_4C powder re-heated with B_2O_3 at 1750 °C using 7C mixture synthesized at 1550 °C.

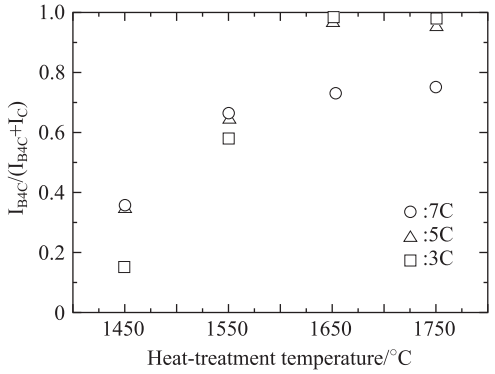

Fig. 8. Change in intensity ratio of the strongest XRD peaks of the products as a function of heat-treatment temperature.

increase in heat-treatment temperature. In the case of heat-treatment at higher temperature using the B_2O_3-rich compositions, edges of polyhedral B_4C particles were rounded off by excess B_2O_3, and it was indicated that a reaction between B_2O_3 and B_4C was proceeded. From these results, heat-treatment temperature and the starting compositions of raw mixtures (the amount of B_2O_3) mainly affected B_4C nuclei number along with primary particle size and morphology of primary B_4C particles, respectively.

4. Conclusions

B_4C powder was synthesized by carbothermal reduction method using B_2O_3 and carbon black mixtures as raw materials and the effects of heat-treatment temperature and starting compositions of powder mixtures on particle morphology were investigated.

The powder products mainly consisted from B_4C and carbon. The B_4C powder synthesized at 1450 °C consisted from mainly spherical particles and rarely polyhedral particles. The B_4C powder synthesized at 1550 °C was large and changed in morphology from polyhedral (prism and plate) to skeletal shape and particle size increased with an increase in the amount of B_2O_3 of starting mixtures. The B_4C powder synthesized beyond 1650 °C mainly consisted from dendrite-like particles aggregated by small primary particles. Morphology of primary B_4C particles synthesized at 1750 °C changed from polyhedral to rounded shape with increasing the amount of B_2O_3 in the starting mixtures. From these results, heat-treatment temperature and the starting compositions of raw mixtures (the amount of B_2O_3) mainly affected B_4C nuclei number along with primary particle size and morphology of primary B_4C particles, respectively.

References

[1] F. Thevenot, Boron carbide—a comprehensive review, Journal of the European Ceramic Society 6 (1990) 205–225.
[2] D. Zhang, D.N. Mcilroy, Y. Geng, M.G. Norton, Growth and characterization of boron carbide nanowires, Journal of Materials Science Letters 18 (1999) 349–351.
[3] R. Ma, Y. Bando, Investigation on the growth of boron carbide nanowires, Chemistry of Materials 14 (2002) 4403–4407.

[4] J. Wei, B. Jiang, Y. Li, C. Xu, D. Wu, B. Wei, Straight boron carbide nanorods prepared from carbon nanotubes, Journal of Materials Chemistry 12 (2002) 3121–3124.
[5] M. Carlsson, F.J. Garcia-Garcia, M. Johnsson, Synthesis and characterisation of boron carbide whiskers and thin elongated platelets, Journal of Crystal Growth 236 (2002) 466–476.
[6] M. Jazirehpour, H.R. Bahahrvandi, A. Alizadeh, N. Ehsani, Facile synthesis of boron carbide elongated nanostructures via a simple in situ thermal evaporation process, Ceramics International 37 (2011) 1055–1061.
[7] C. Motoc, F. Constantinescu, Growth and thermal etching of boron carbide, Journal of Crystal Growth 18 (1973) 29–33.
[8] C.H. Jung, M.J. Lee, C.J. Kim, Preparation of carbon-free B_4C powder from B_2O_3 oxide by carbothermal reduction process, Materials Letters 58 (2004) 609–614.
[9] A. Alizadeh, E. Taheri-Nassaj, N. Ehsani, Synthesis of boron carbide powder by a carbothermic reduction method, Journal of the European Ceramic Society 24 (2004) 3227–3234.
[10] A.W. Weimer, W.G. Moore, R.P. Roach, J.E. Hitt, R.S. Dixit, S.E. Pratsinis, Kinetics of carbothermal reduction synthesis of boron carbide, Journal of the American Ceramic Society 75 (1992) 2509–2514.
[11] A. Sinha, T. Mahata, B.P. Sharma, Carbothermal route for preparation of boron carbide powder from boric acid-citric acid gel precursor, Journal of Nuclear Materials 301 (2002) 165–169.
[12] A.M. Hadian, J.A. Bigdeloo, The effect of time, temperature and composition on boron carbide synthesis by sol-gel method, Journal of Materials Engineering and Performance 17 (2008) 44–49.
[13] S. Mondal, A.K. Banthia, Low-temperature synthetic route for boron carbide, Journal of the European Ceramic Society 25 (2005) 287–291.
[14] I. Yanase, R. Ogawara, H. Kobayashi, Synthesis of boron carbide powder from polyvinyl borate precursor, Materials Letters 63 (2009) 91–93.
[15] M. Kakiage, N. Tahara, I. Yanase, H. Kobayashi, Low-temperature synthesis of boron carbide powder from condensed boric acid-glycerin product, Materials Letters 65 (2011) 1839–1841.
[16] M. Kakiage, N. Tahara, S. Yanagidani, I. Yanase, H. Kobayashi, Effect of boron oxide/carbon arrangement of precursor derived from condensed polymer-boric acid product on low-temperature synthesis of boron carbide powder, Journal of the Ceramic Society of Japan 119 (2011) 422–425.
[17] M.G. Inghram, R.F. Porter, W.A. Chupka, Mass spectrometric study of gaseous species in the B-B_2O_3 system, Journal of Chemical Physics 25 (1956) 498–501.
[18] V.D. Derkach, S.P. Gordienko, B.V. Fenochka, A.P. Epik, N.F. Kolesnik, Composition of the gaseous phase over the system B_4C-B_2O_3, Powder Metallurgy and Metal Ceramics 10 (1971) 301–303.